The 2010 IEEE/RSJ International Conference on
Intelligent Robots and Systems
October 18-22, 2010, Taipei, Taiwan

Development of Knee Power Assist using Backdrivable Electro-Hydrostatic Actuator

Hiroshi Kaminaga, Tomoya Amari, Yamato Niwa, and Yoshihiko Nakamura

Abstract— **Backdrivability is a keyword with rising importance, not only in humanoid robots, but also to wearable robots. Power assist robots, namely exoskeletons are expected to provide mobility and independence to elderly and people with disability. In such robots, without backdrivability, error between human and robot motion can be painful; sometimes dangerous. In this research, we apply a type of hydraulic actuator, specially designed to realize backdrivability, to exoskeletal robot to improve backdrivability. We present the basic methodology to apply such hydraulic actuator to wearable robots. We developed prototype of knee joint power assist exoskeleton and performed fundamental tests to verify the design method validity.**

I. Introduction

The actuator property "*backdrivability*" is getting increasingly important in field of robotics, mainly for robots interacting with human, that needs to realize low impedance. Wearable robots including exoskeletons and prosthetics are not exceptions. Exoskeletons must not impede the movement of subject. Prosthetics must not damage environment when it collides with surroundings by accident. To realize those safety and comfort features, realization of low mechanical impedance is necessary.

Traditionally, robot actuators were built non-backdrivable. One of the reasons is that backdrivability was not necessary when the achievement of high position accuracy was the objective of robots. Gear drives including harmonic drive gears and valve controlled hydraulic drives are common robot actuators, but they are rarely backdrivable.

As an attempt to make non-backdrivable actuator backdrivable, admittance control [1] is widely used. In admittance control, external force is measured with force sensor and fed back to motor to emulate backdriving behavior. Since the backdrivability is emulated, the effective frequency range of mechanical impedance reproduction is limited by controller bandwidth. Hence it is desirable to realize backdrivability mechanically for safe and reliable operation. [2], [3].

Series Elastic Actuators (SEAs)[4] are attempts to make actuator system backdrivable with non-backdrivable actuator. RoboKnee by Pratt et al. [5] and IHMC Mobility Assist Exoskeleton by Kwa et al. [6] are examples of exoskeleton using SEAs. However, SEAs have tendency of being heavy and bulky since they need additional elastic components to realize natural elasticity. SEAs also have limited actuator placement freedom since all components are mechanically coupled. It makes actively driven joints even larger, making it obstacle. Furthermore, SEAs have difficulty in maintaining controllability when higher backdrivability is pursued [7].

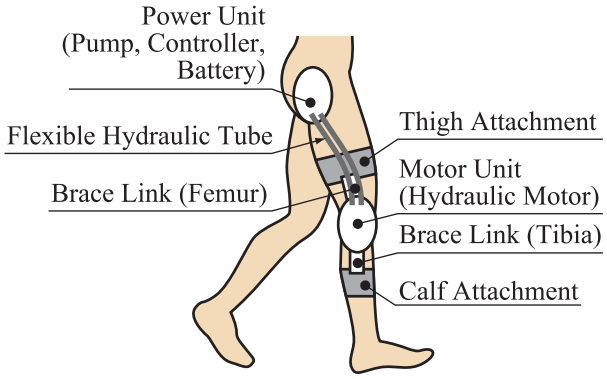

Fig. 1. Concept of Knee Power Assist with EHA

Sulzer et al. [8] proposed SERKA (Series Elastic Remote Knee Actuator) that drive spring coupled joint by remotely placed motor with wire tendon. By placing the heavy motor remote, mass of extremity becomes lighter, which enhances the comfort. It showed effectivity of remote placement of heavy objects, but still trade-off relation of controllability and backdrivability is not resolved.

EHAs (Electro-Hydrostatic Actuators) are displacement type hydraulic actuators. With appropriate design, whole actuator system becomes backdrivable as in [9], [10]. We [10] introduced the idea of output backdrivability and total backdrivability to explain the backdriving states in general actuators including hydraulic drives. Also, placement of actuator has large degree of freedom as in [9] since the force transmission is done with hydraulic oil. Furthermore, EHAs are very durable that ensures the safety of the exoskeleton. Efficiency of EHA is very high among the hydraulic systems because there is no waste energy being turned into heat at the valves and regulators. This is major advantage against the system using valve controlled hydraulic system such as [2]. Since EHA is a SDA (Series Dissipative Actuator) [7] actuator, we can also overcome the issue of trade-off between backdrivability and controllability.

From these reasons, we can expect EHA to be suitable

This work was supported partially by Grant-in-Aid for Scientific Research (No.20-10620) for Research Fellowships of the Japan Society for the Promotion of Science for Young Scientists and partially by "IRT Foundation to Support Man and Aging Society" under Special Coordination Funds for Promoting Science and Technology from MEXT.

H. Kaminaga, T. Amari, Y. Niwa, and Y. Nakamura are with Department of Mechano-Informatics, The University of Tokyo, 7-3-1 Hongo, Bunkyo-Ku, Tokyo 113-8656, Japan {kaminaga, amari, niwa, nakamura}@ynl.t.u-tokyo.ac.jp

actuator in exoskeletons, and usage of EHAs in exoskeleton would make fundamental difference in usability and performance using other types of actuators as gear drives and conventional hydraulics

In this research, our objective is to develop an EHA driven exoskeleton for lower extremity; mainly targeted for elderly. To start with, we developed the power assist exoskeleton for knee joint. Actual specification is based on human motion analysis and statistical data of Japanese elderly, but the proposed method can be applied in general case with appropriate statistical data. In this paper, we explain the methodology for applying EHA to power assist device; power requirement estimation, mechanical design, and basic control strategy is explained. Also, basic tests on developed prototype is performed.

II. Specification of Exoskeleton

A. CS-30 Test Criterion

To improve the ability of locomotion, we must consider sequence of motion included in locomotion. In general, locomotion can be expressed as a package of motion as:

1) resting position $\rightarrow$ walking position (Phase I)
2) walking (Phase II)
3) walking position $\rightarrow$ resting position (Phase III)

The ability of motion is easily lost in elderly due to lack in log joint torque. We must resolve this limiting factor mainly in phase I and III, due to its large requirement in torque, to improve locomotion ability as whole. We take following approach as power assist strategy.

1) torque oriented support in phase I and III
2) speed oriented support in phase II

It is difficult to discuss about necessary knee torque only by its value. As a measure of independence in elderly, we focused on a report that there is a correlation between score of CS-30 test and excretion independence, one of the largest importance in improving quality of life. CS-30 test, originally proposed by Jones et al. [11] and modified by Nakatani et al. [12], is a test that measure number of standing up completed from a chair in 30 seconds. It is reported that for Japanese elderly to be independent, it is important that the subject can complete more than 6 stand-ups in CS-30 test [13] for excretion independence. In this research, we put our objective on supporting subject so he or she can mark more than 10 times in CS-30 test. [1]

It is reported that the test result in CS-30 test and maximum lower limb extension force (1RM: Repetition Maximum) have correlation [14]. Extrapolating the data of [14], it is expected so extension force of 1RM=200(N) to score 10 times in CS-30 test. According to the Human Characteristics Database [15], healthy Japanese elderly aged from 65-80 years old, with sample number of 510, have average weight of 56.8(kg) (The standard deviation is 9.0(kg)). This means to score 10 in CS-30 test, 35% of the body weight must be supported.

[1]We must be precise that we focus on providing enough support in torque to subject to score more than 10 times, not the speed. We do not focus on speed requirement for realizing the score.

TABLE I
Captured Motions

Motion	Iteration
Standing Up from 600mm Chair	20
Standing Up from 500mm Chair	20
Standing Up from 300mm Chair	20
Walk Forward	6

The average isometric lower limb extension force estimated from [15] is 567.4(N) and minimum is 150.5(N). That means in the worst case, only 27% of the body weight can be supported by examinee's own leg. Since 1RM is measured in isokinetic contraction, which is about 78% of isometric contraction force [16], about 15% of the body weight must be supported externally to enable all examinees to mark 10 in CS-30 test.

Since the deviation of muscle force of elderly are very large, safety factor of 2 was selected for this research. Exoskeleton to be designed will support 30% of the average body weight, which corresponds to 166(N) of leg extension force. We neglect the weight of the exoskeleton device now because we are developing single joint exoskeleton, which is expected to be less than 5% of the body weight.

B. Power Requirement Estimation by Human Motion Analysis

To specify necessary performance of the exoskeleton, we need to know not only the torque but time series relationship between torque and speed because the actuator output torque is dependent on the speed. Optical motion capturing was used to record the movement of subject. We used 35 optical passive markers attached on healthy subject who performed specified movement to record healthy nominal movement. Recorded movements were fit to 34 DOF human figure with weight of 71(kg). By performing inverse kinematics and inverse dynamics, joint angle and joint torque were computed. Three dimensional marker position was recorded each 5(msec), floor reaction force was recorded each 1(msec).

Locomotion in daily life generally require standing up from chair (or floor), walking, and sitting down. Considering the sequence, movements performed by subject was selected as in Table I. Exoskeleton being designed must satisfy design criterion for all the movements in Table I.

Among the joints of lower extremity, hip joint, knee joint, and ankle joint, knee joint produces large torque and disorders such as osteoarthritis are likely to happen due to aging. Knee buckling while walking causes fall on the back, which have very high risk of serious injury. In this paper, we focus on the knee joint.

Inverse dynamics computation was used to analyze the captured motion data. The results are shown in figures from Fig. 2 to Fig. 4. An example of time trajectories of knee angle and torque is shown in Fig. 4.

From Fig. 2, it can be seen that as the height of the chair from standing up becomes lower, necessary torque increases.

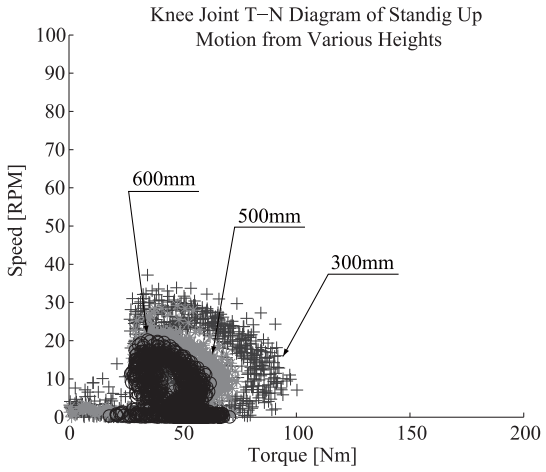

Fig. 2. Torque-Speed Plot of Stand up Motion

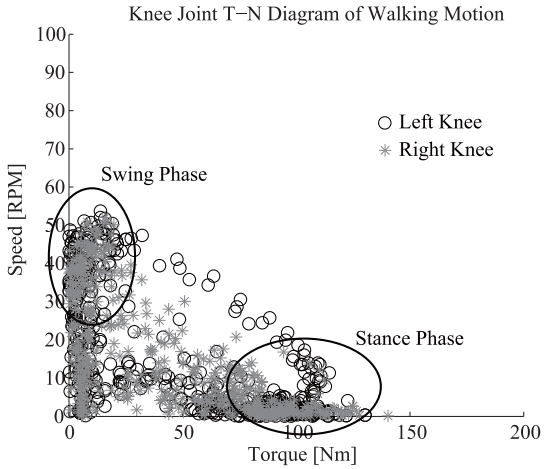

Fig. 3. Torque-Speed Plot of Walking Motion

From the experiment, torque and speed needed for standing up from chair of 300(mm) high, which required most torque, maximum of 100(Nm) is needed. When the maximum torque is necessary, speed of 10(RPM) is needed.

From Fig. 3, we can see the difference in necessary characteristics of knee during stance phase and swing phase. Maximum torque is necessary in stance phase. However, knee is locked at the end of moving range in the case of human to the direction of extension. This can be seen from Fig. 4. This means, no big supporting torque is needed in this case. On the other hand, during the swing phase, output torque is small but the speed is large. This speed must be satisfied in order for the exoskeleton to be not a obstacle while walking. From Fig. 3, maximum speed of 55(RPM) is needed with torque of 20(Nm) for supporting walking.

The human figure used in dynamics computation was 71(kg). We scale the result of the dynamics computation by 80% to fit the body weight to the average body weight of elderly. The necessary specification becomes as shown in Table II.

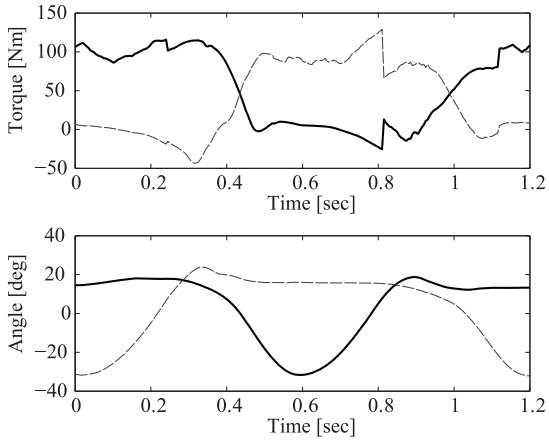

Fig. 4. Transition of Knee Torque and Angle During Walking Forward with Frequency of 0.83(Hz). Solid line show data of left knee and dashed line show data of right knee. Glitches in the upper figure are spurious due to the contact condition misdetection at leg exchange.

TABLE II
REQUIRED SPECIFICATION OF THE KNEE SUPPORT

Description	Value	Note
Maximum Torque	30(Nm)	at 10(RPM)
Maximum Speed	55(RPM)	at 0(Nm)(external)

III. MECHANICAL DESIGN

A. Design Concept

Our objective for this paper is to develop a single joint power assist exoskeleton for the knee joint. We focused on EHA as a actuator for power assist exoskeleton for following properties:

1) Force controllability. Since the actuator is backdrivable, we have more sensitivity and control over force control.
2) Durability. In hydraulic system, force is transmitted with large surface area, which disturbs stress and enhances the durability.
3) Actuator placement freedom. In hydraulic system, there is placement freedom for pump placement. Also relative position between pump and hydraulic motor can be flexible. Heavy devices can be placed near the center of mass to enhance mobility.

Fig. 1 shows the concept diagram of the exoskeleton to develop. Hydraulic portion of EHA is attached to the knee and rest of the portion as pump, controller, and battery are attached to hip. We name the linkages connecting attachment part and EHA, brace links. We must realize the structure that is compliant to the human movement, and hopefully, easy to attach and detach.

Following two issues are few of the largest challenges in using EHA as an actuator for exoskeleton.

1) Avoiding oil leakage without degrading backdrivability.
2) Realizing small and light system.

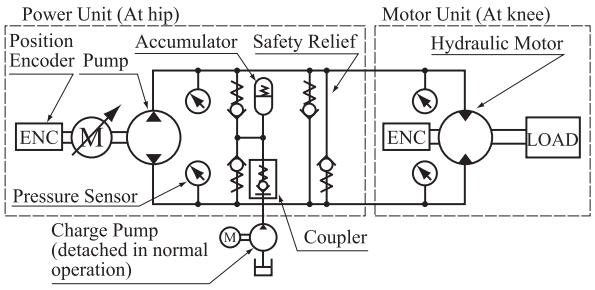

Fig. 5. Structure of Electro-Hydrostatic Actuator

TABLE III
NOMENCLATURE

Symbol	Description (units)	
	Prismatic	Revolute
θ_i	Position (m)	Angular position (m)
J_i	Mass (kg)	Moment of inertia ($\mathrm{kg \cdot m^2}$)
τ_f^i	Friction force (N)	Friction Torque (Nm)
τ_i	Input force (N)	Input torque (Nm)
p_i	Pressure difference (Pa)	
$\bar{p}$	Amount of pressurization (Pa)	

To realize compliant mechanism, we introduced passive joints in series to the active joint driven by EHA. To realize low friction without leakage, oil seal evaluation was performed using a test rig. To realize small and light system, we designed hydraulic system that can bare higher operating pressure than that of our previous works[9], [10].

B. Model Based Output Power Estimation for Electro-Hydrostatic Actuator

EHAs are displacement type hydraulic actuator having structure as in Fig. 5. Usually one pump is connected to one hydraulic motor without servo valves. The coupling between components in EHA are hydraulic and have internal leakage. This makes the system behavior more complicated because the velocity relations are not conserved. To make the output power estimation for such system, we need to take model based approach. The system dynamics of an EHA is given as in (1) [10].

$$\begin{aligned} J_i\ddot{\theta}_i &= -k_3^i p_i - \tau_f^i(\dot{\theta}_i, p_i, \bar{p}) + \tau_i \\ &= -k_1^i k_3^i \dot{\theta}_i + k_2^i k_3^i \dot{\theta}_{\bar{i}} - \tau_f^i(\dot{\theta}_i, \dot{\theta}_{\bar{i}}, \bar{p}) + \tau_i \end{aligned} \quad (1)$$

Here, subscript and superscript i denotes either p (pump) or m (motor). $\bar{i}$ denotes opposite of i. See Table III for the parameter meanings. $k^i_{\{1,2,3\}}$ are constants.

The relationship between pressure p_i and speed $\dot{\theta}_i$ is given as follows.

$$p_i = k_1^i \dot{\theta}_i - k_2^i \dot{\theta}_{\bar{i}} \quad (2)$$

Output characteristics of EHA at steady-state, or when $\ddot{\theta}_i = 0$ can be solved for actuator output speed and torque in closed form under the condition of $\dot{\theta}_p, \dot{\theta}_m, p_p > 0$ and $p_m < 0$, thus in forward driving condition [10].

Using more detailed notation in [7], and under assumption that the nonlinear friction at bearing is negligible, positive direction ($\dot{\theta}_p > 0$) forward drive steady state output torque and speed are given as follows:

$$\begin{bmatrix} \dot{\theta}_m \\ \tau_m \end{bmatrix} = \begin{bmatrix} A_1 & 0 \\ A_2 & 1 \end{bmatrix}^{-1} \left(\begin{bmatrix} B_1 & -1 \\ B_2 & 0 \end{bmatrix} \begin{bmatrix} \dot{\theta}_p \\ \tau_p \end{bmatrix} + \begin{bmatrix} k_{cs}^p \left(p_{s0}^p + \bar{p}\right) \\ k_{cs}^m \left(p_{s0}^m + \bar{p}\right) \end{bmatrix} \right) \quad (3)$$

where

$$\begin{aligned} A_1 &= \left(k_3^p + k_{cbr}^p\right) k_2^p \\ A_2 &= -k_3^m k_1^m - k_v^m \\ B_1 &= \left(k_3^p + k_{cbr}^p\right) k_1^p + k_v^p \\ B_2 &= -k_3^m k_2^m \end{aligned}$$

k_{cbr}^p is a constant mainly containing friction at mesh of trochoid gears in the pump, and k_v^i is a constant including all viscous friction coefficients. k_{cs}^i is Coulomb friction coefficient at oil seal, and p_{s0}^p is pressure acting between axis and oil seal at $\bar{p} = 0$ caused by elasticity of oil seal.

Using (3), we can estimate the resulting torque-speed relation from motor characteristics.

TABLE IV
EHA DESIGN PARAMETER

Description	Value	
Motor rated output	100	(W)
Oil Viscosity	100	(cSt)
Maximum operating pressure	4.6	(MPa)
Total reduction ratio	449	
Pump displacement	360	($\mathrm{mm^3/rev}$)
Hydraulic motor displacement	24000	($\mathrm{mm^3/rev}$)

C. Actuator Design

Since the knee joint of human basically is a hinge joint, we chose the rotary output hydraulic motor. This way we can minimize the chance of exoskeleton being an obstacle. As pump, we chose trochoid type inner gear pump from its large displacement per pump size. As hydraulic motor, we chose double vane motor, which can produce large torque with same pressure relative to its package volume. Friction parameters for oil seals were identified with a test rig. See Table IV for design specification.

In our previous work [10], we chose flange type connection for EHA output axis. However, usage of flange output resulted in large oil seal diameter, which increased friction torque. To further enhancement of backdrivability, we needed to reduce this friction torque. In this research, we chose axis type output to reduce diameter of the oil seal, but this was a design challenge because with smaller diameter to transmit the torque, easier it is to cause the slippage.

Pressurization is vital in closed circuit hydraulic system as EHA to avoid cavitation[17]. To avoid cavitation, minimum hydraulic pressure in the system must be sufficiently high; this is called pressurization. Charge pump is used to give pressurization to closed circuit upon assembly of the system as in Fig. 5. However, in normal operation, charge pump is not necessary if amount of pressurization is kept. In this

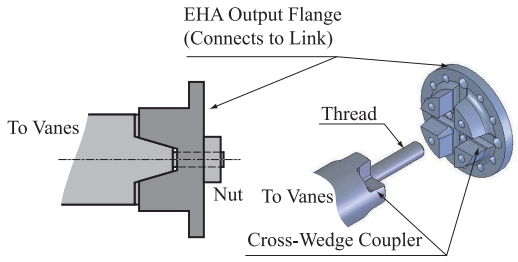

Fig. 6. Cross-Wedge Coupler. Left figure is the conceptual sketch. Thread and nut gives enough stress on the wedge coupler to eliminate backlash. Threaded axis also serves as centering axis. Link is attached to the flange with sufficient surface area to transmit the torque. Right figure shows the designed coupler.

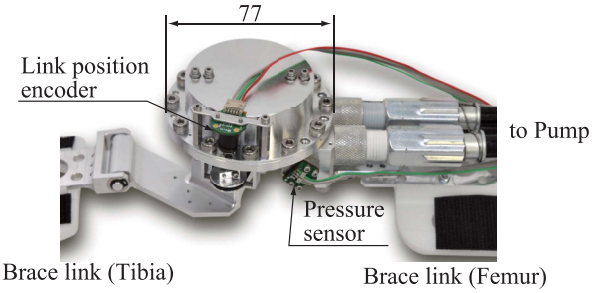

Fig. 7. Outlook of Developed Hydraulic Motor

research, we developed miniature accumulator that enables us to detach charge pump to reduce weight of the system in normal operation.

Fig. 7 shows developed vane motor and Fig. 8 shows developed pump. Hydraulic motor assembly is equipped with motor side pressure sensor. Pump assembly is equipped with pump side pressure sensor, accumulator, charge circuitry, and safety relief circuitry.

D. Peripheral Design

Anatomic structure of the knee joint is a pair of bones bound together with ligaments as shown in Fig. 9. Although macroscopic movement of the knee is approximated by single hinge joint, real movement is very complicated due to the bone structure and ligament interactions. One of those movements is called screw-home movement[18]; tibia

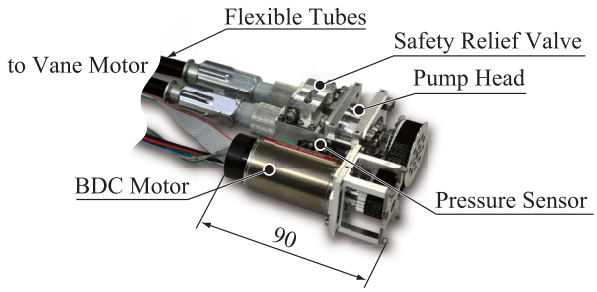

Fig. 8. Outlook of Developed Pump. Miniature accumulator and connection to charge pump is on the bottom side.

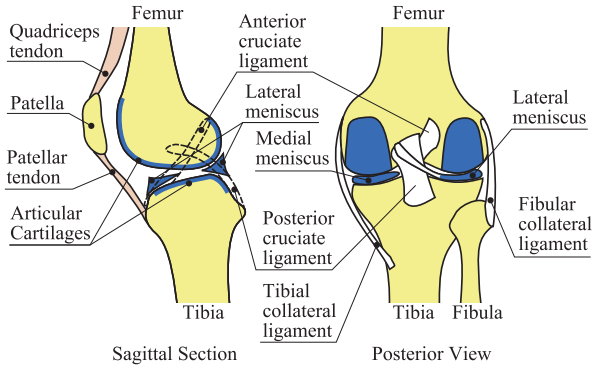

Fig. 9. Anatomic Structure of Knee[20]. The figure depicts the structure of right knee.

TABLE V
KNEE MOVEMENT IN FLEXION/EXTENSION [19]

Description	Range	
Lateral/Medial Rotation	20.2	(deg)
Varus/Valgus Rotation	4.3	(deg)

rotates against femur in lateral and medial direction while the knee joint flexes and extends. This movement is present for everyone including healthy subject and must not be impeded by exoskeleton. There is also varus and valgus movements of tibia in knee flexion/extension. From the statistics[19], we need movement range of the value shown in Table V.

In this research, we place two passive joints in brace links to allow these movements. Passive joint axes are placed perpendicular to the EHA axis as in Fig. 10.

Thigh and calf attachments are the direct interface to human, so care must be taken upon material selection to satisfy human skin compatibility. In this research we utilized the attachment mechanism of existing knee brace supporter for knee injury. In this supporter, attachment to thigh and calf is done by wrapping thigh or calf with neoprene rubber band with Velcro. Brace links were designed to fit into these bands. Fig. 11 shows the structure of brace links with passive joints. Fig. 12 shows the motor unit assembly (EHA attached to brace links and thigh/calf attachments) of the developed exoskeleton. Fig. 13 shows the developed knee power assist attached to lower limb.

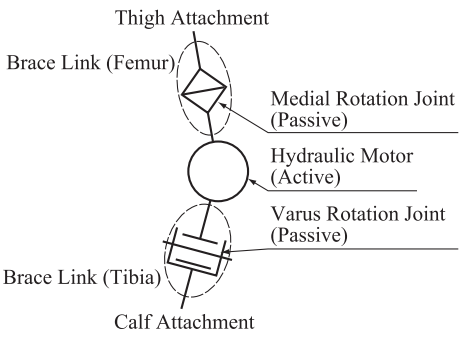

Fig. 10. Joint Arrangement of Exoskeleton

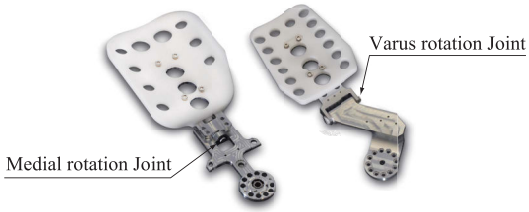

Fig. 11. Structure of Brace Links with Passive Joints

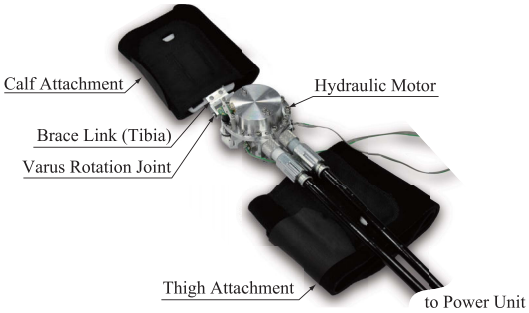

Fig. 12. Developed Motor Unit Assembly. Brace link for femur is on bottom side.

IV. Experiments

A. Intrinsic Backdrivability

Realization of high backdrivability is necessary in realizing force sensitive robot systems. Advantage of EHA is that it can realize output backdrivability regardless of reduction ratio. This is a significant advantage against mechanical transmissions as gear drives. However, ease of backdriving is heavily dependent on oil seal friction at output axis of EHA because this friction cannot be measured and controlled without external torque sensor. We are targeted for wearable system, so we cannot include additional weight of torque sensor, which is not negligible.

In our previous study [10], we suffered from this friction torque. In the designed EHA, because we developed cross-wedge backlash-less coupler, we succeeded in significant reduction of the friction [2]. We used the test apparatus shown in Fig. 14 for backdrivability evaluation.

Test results are shown in Table VII. As the result, we confirmed output backdrivability was less than 200(mNm).

[2]It should be noted that cross-wedge coupler might not be the optimal solution in other scales. In the scale of exoskeleton for knee, this solution was confirmed to be reasonable with finite element method analysis.

TABLE VI
Mass of Wearable Robot System

Part	Mass	
Pump	299.6	(g) (Dry Weight, Design Value)
Motor	541	(g) (Dry Weight, Design Value)
Total	1124	(g) (With Oil, Measured Value)

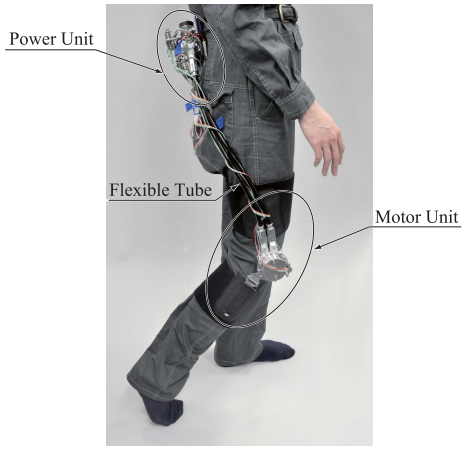

Fig. 13. Developed Knee Power Assist Driven with Backdrivable Electro-Hydrostatic Actuator

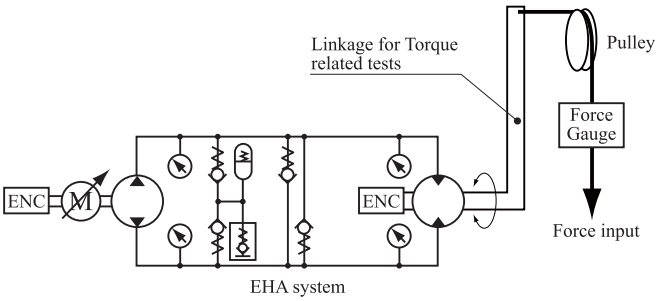

Fig. 14. Test Apparatus for Backdrivability Test and Impedance Control Evaluation

Actual output backdriving torque is smaller, but with the combination of link side encoder resolution, force gauge resolution, and test arm length (moment arm), 200(mNm) was the measurement resolution. Total backdriving torque exceeds calculated value largely at the pressurization of 1.5(MPa). We scaled the data we observed the test rig (Fig. 15), which has the axis diameter of 18(mm). We scaled the friction parameter to oil seal with other diameter under an assumption that the friction value per unit surface area at contact is constant regardless of the seal size. It is expected that this simple scaling was inaccurate. EHA output axis diameter is 15(mm), so this error is small, but the pump

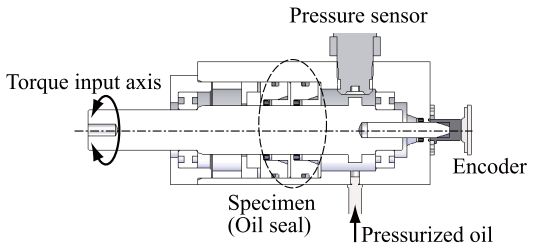

Fig. 15. Apparatus for Oil Seal Friction Identification[21]. Torque applied to the axis was measured with force gauge for static friction test and motor current for dynamic friction test.

TABLE VII

COMPARISON BETWEEN CALCULATED AND MEASURED BACKDRIVE TORQUE[21]

Pressurization(MPa)	0.5	1.0	1.5
Measured Output Backdrive Torque (Nm)	less than 0.2		
Expected Output Backdrive Torque (Nm)	0.037	0.038	0.040
Measured Total Backdrive Torque (Nm)	1.3	2.2	4.8
Expected Total Backdrive Torque (Nm)	1.6	1.9	2.2

TABLE VIII

COMPARISON OF BACKDRIVE TORQUE BETWEEN DEVELOPED EHA AND HUMANOID KNEE JOINT EHA IN [10]

Description	Developed EHA	Humanoid Knee Joint EHA[10]
Output Backdrive Torque (Nm)	less than 0.2	6.2
Total Backdrive Torque (Nm)	1.3	7.5
Simulated Maximum Continuous Output Torque (Nm)	35	120
Ratio of Output Backdrive Torque to Maximum Output Torque (%)	0.57	5.1

axis diameter is 4(mm) which might have different friction characteristics from the oil seal used in identification. What is observed from the test result is that the pump axis oil seal friction torque is more sensitive to the pressurization than what we expected. At pressurization of 0.5(MPa) and 1.0(MPa), the test results show good fit to the expected data.

As in Table VIII, there is significant improvement in backdrivability even taking in account about maximum torque.

B. Impedance Control

To evaluate the force sensitive behavior of the developed actuator, impedance control was implemented. We used same control strategy as in [10] and [7]. Apparent inertia was scaled down to 1/5 of physical inertia by torque feedback using pressure sensor. Virtual impedance was realized by measuring the deflection of the link position from resting position and exerting appropriate torque.

Fig. 16 shows the impedance control result for different desired stiffness. The result show good fit to the desired stiffness value. Fig. 17 shows the result for pressurization of 1.5(MPa). From the same reason as in previous section, pump friction is larger than what we expected, that caused the error in torque in large toque range for high pressurization case. This is one of the drawback of using impedance control instead of admittance control since admittance control measure force and control position thus there is less effect of friction. However, in reality, stability of the control system has much higher priority than realizing exact stiffness. Furthermore, by identifying friction parameter for smaller diameter oil seals with appropriate diameter test rig, we should get much more accurate result.

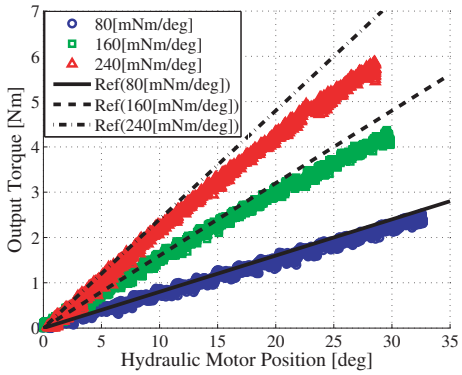

Fig. 16. Impedance Test Result under Pressurization of 1.0(MPa). Ref shows the behavior of ideal system with desired stiffness value.

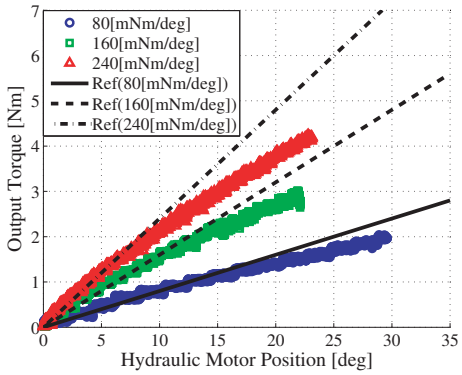

Fig. 17. Impedance Test Result under Pressurization of 1.5(MPa). Ref shows the behavior of ideal system with desired stiffness value.

C. Comfort Test

To evaluate the effect of the passive joints on comfort, normal force acting between brace link and body was examined. Forces were measured at 4 corner points on interface surface of each brace links, resulting 8 points of force measurements. At the same time, knee flexion angle was measured. As comfort index, force of the point giving largest deviation over time was selected. In equation, force being evaluated is given as follows:

$$f_{max}(t) = f_j(t) \tag{4}$$

where

$$j = \arg\max_i \int_0^t (f_i(\xi) - \bar{f}_i)^2 d\xi \tag{5}$$

$$\bar{f}_i = \frac{1}{t}\int_0^t f_i(\xi) d\xi \tag{6}$$

The test was performed on a healthy subject of 22 years old. Multiple squatting motions were performed. Fig. 18 shows the evaluation result with and without passive joints. As a result, maximum normal force was observed at upper anterior sensor placed in femur brace link. When there is no passive joint, maximum force of brace link pushing against thigh was 38(N), where it was relieved to 6(N) with passive joint. This is a significant reduction and expected to reduce

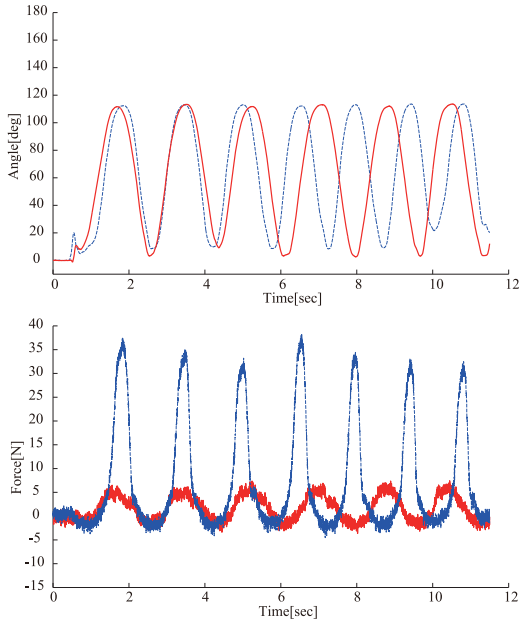

Fig. 18. Reduction of Link Force Pressing Against Leg by Passive Joints. Dashed blue line shows the force of brace link pressing against thigh without passive joint. Solid red line shows the result with passive joints.

the chance of discomfort and pain due to the usage of exoskeleton.

V. Conclusion

In this paper, we reported the methodology of developing knee joint power assist exoskeleton using backdrivable electro-hydrostatic actuator. Followings are the conclusions:

1) Torque and speed required for locomotion including standing up and walking for a person weighing 71 (kg) is 100 (Nm) and 55 (RPM).
2) Scoring more than 10 times in CS-30 test was selected as an index for the independence of elderly. For vast majority of elderly to score more than 10, support of 30% of body weight is necessary. Torque of 30 (Nm) and speed of 55 (RPM) is requirement for exoskeleton for such support.
3) Design concept of splitting EHA to power unit and motor unit was presented. System driven with 100 (W) brushless DC motor was designed to meet above specification. All range of specification can be covered with continuous operating region. Total system weight is 1124(g) including all components but battery. We also proposed the method to add two passive joints to reduce the stress acting on the exoskeleton attachment from anatomic knee movement. Disturbing force was reduced to almost 1/6 by the introduction of passive joint.
4) By structural refinement, we succeeded in realizing the output backdrivability at 0.5(%) of maximum torque, which is the significant improvement from previous work. From the basic test on the oil seals, we confirmed there is no leakage from the oil seal with this configuration.

References

[1] N. Hogan, "Impedance Control: An Approach to Manipulation: Part I-III," *Trans. of ASME J. Dyn. Sys. Meas. Ctrl*, vol. 107, no. 1, pp. 1–23, 1985.

[2] A. B. Zoss, H. Kazerooni, and A. Chu, "Biomechanical Design of the Berkeley Lower Extremity Exoskeleton (BLEEX)," *IEEE/ASME Trans. on Mechatronics*, vol. 11, no. 2, pp. 128–138, 2006.

[3] T. Hayashi, H. Kawamoto, and Y. Sankai, "Control method of robot suit hal working as operator's muscle using biological and dynamical information," in *Proc. of the IEEE/RSJ Int'l Conf. on Intelligent Robots and Systems*, 2005, pp. 3063 – 3068.

[4] G. A. Pratt and M. M. Williamson, "Series Elastic Actuators," in *Proc. of IEEE/RSJ Int'l Conf. on Intelligent Robots and Systems*, vol. 1, 1995, pp. 399–406.

[5] J. E. Pratt, B. T. Krupp, C. J. Morse, and S. H. Collins, "The RoboKnee: An Exoskeleton for Enhancing Strength and Endurance During Walking," in *Proc. of IEEE Int'l Conf. on Robotics and Automation*, 2004, pp. 2430–2435.

[6] H. K. Kwa, J. H. Noorden, M. Missel, T. Craig, J. E. Pratt, and P. D. Neuhaus, "Development of the ihmc mobility assist exoskeleton," in *Proc. of IEEE Int'l Conf. on Robotics and Automation*, 2009, pp. 2556–2562.

[7] H. Kaminaga, T. Amari, Y. Katayama, J. Ono, Y. Shimoyama, and Y. Nakamura, "Backdrivability Analysis of Electro-Hydrostatic Actuator and Series Dissipative Actuation Model," in *Proc. of IEEE Int'l Conf. on Robotics and Automations*, 2010, pp. 4204–4211.

[8] J. S. Sulzer, R. A. Roiz, M. A. Peshkin, and J. L. Patton, "A Highly Backdrivable, Lightweight Knee Actuator for Investigating Gait in Stroke," *IEEE Trans. on Robotics*, vol. 25, no. 3, pp. 539–548, 2009.

[9] H. Kaminaga, T. Yamamoto, J. Ono, and Y. Nakamura, "Anthropomorphic Robot Hand With Hydrostatic Actuators," in *Proc. of 7th IEEE-RAS Int'l Conf. on Humanoid Robots*, 2007, pp. 36–41.

[10] H. Kaminaga, J. Ono, Y. Nakashima, and Y. Nakamura, "Development of Backdrivable Hydraulic Joint Mechanism for Knee Joint of Humanoid Robots," in *Proc. of IEEE Int'l Conf. on Robotics and Automations*, 2009, pp. 1577–1582.

[11] C. J. Jones, R. E. Rikli, and W. C. Beam, "A 30-s Chair-Stand Test as a Measure of Lower Body Strength In Community-Residing Older Adults," *Res. Q. Exerc. Sport*, vol. 70, pp. 113–119, 1999.

[12] T. Nakatani, M. Nadamoto, K. Mimura, and M. Itoh, "Validation of a 30-sec Chair-Stand Test for Evaluating Lower Extremity Muscle Strength in Japanese Elderly Adults," *Japan J. Phys. Educ. Hlth. Sport Sci.*, vol. 47, pp. 451–461, 2002.

[13] T. Sugihara, S. Mishima, K. Takeda, T. Funayama, M. Naganuma, M. Tanaka, E. Ochiai, M. Takagi, and E. Tsushima, "Elderly Peoples' Stand Up Ability and Excretion Independence," *Rigakuryoho Kagaku*, vol. 22, no. 1, pp. 89–92, 2007, in Japanese.

[14] K. Nakahara, "Relationships between the 30-second Chair-Stand Test Given to Elderly People and the Maximum Extension Strength of Lower Limbs as well as the Functioning of Daily Living," *Rigakuryoho Kagaku*, vol. 22, no. 2, pp. 225–228, 2007, in Japanese.

[15] National Institute of Technology and Evaluation, "Human Characteristics Database," http://www.tech.nite.go.jp/human/jp/contents/cindex/database.html in Japanese.

[16] M. P. Murray, G. M. Gardner, L. A. Mollinger, and S. B. Sepic, "Strength of Isometric and Isokinetic Contractions," *Physical Therapy*, vol. 60, no. 4, pp. 412–419, 1980.

[17] J. E. Bobrow and J. Desai, "Modeling and Analysis of a High-Torque, Hydrostatic Actuator for Robotic Applications," *Experimental Robotics*, pp. 215–228, 1989.

[18] L. G. Hallen and O. Lindahl, "The "Screw-Home" Movement in the Knee Joint," *Acta Orthopaedica*, vol. 37, pp. 97–106, 1966.

[19] H. Kurosawa, P. S. Walker, S. Abe, A. Garg, and T. Hunter, "Geometry and Motion of the Knee for Implant and Orthotic Design," *J. Biomechanics*, vol. 18, no. 7, pp. 487–499, 1985.

[20] J. C. Thompson, *Netter's Concise Orthopeadic Anatomy*, 2nd ed. Saunders, 2010.

[21] H. Kaminaga, T. Amari, Y. Niwa, and Y. Nakamura, "Electro-Hydrostatic Actuators with Series Dissipative Property and their Application to Power Assist Devices," in *Proc. of IEEE/RAS-EMBS Int'l Conf. on Biomedical Robotics and Biomechatronics*, 2010, in print.